

# Synthesis, physical-chemical and biological properties of amphiphilic amino acid conjugates of nitroxides†

Grégory Durand,\*<sup>a</sup> Fanny Choteau,<sup>a</sup> Robert A. Prosak,<sup>b</sup> Antal Rockenbauer,<sup>c</sup> Frederick A. Villamena\*<sup>bd</sup> and Bernard Pucci<sup>a</sup>

Received (in Montpellier, France) 13th January 2010, Accepted 18th March 2010

DOI: 10.1039/c0nj00024h

Due to the dual property of synthetic nitroxide compounds to either act as probe or antioxidant, efforts toward their selective targeting using specific ligands have been extensively explored. Herein, we report the synthesis of novel amphiphilic nitroxides in which the nitroxyl group is grafted onto an amphiphilic carrier comprising a lactobionamide polar group, a non-polar alkyl chain and an amino acid as scaffold. Piperidine and pyrrolidine nitroxides such as 4-amino-TEMPO (4-AT) and 3-carboxypropyl (3-CP), respectively, were grafted onto the amphiphilic carriers. To further investigate the effect of the nature of the chain on the physical-chemical and biological properties of nitroxides, hydrogenated or perfluorinated alkyl chains were used. The self-aggregation properties in aqueous media of these surfactant-like nitroxides were confirmed by dynamic light scattering (DLS) as well as electron paramagnetic resonance (EPR) spectroscopy, and were correlated with their respective lipophilicity. The effect of the carrier groups on the electrochemical property of nitroxides was investigated using cyclic voltammetry, and the rates of reduction using ascorbate as reducing agent were measured. Finally, their cytoprotective property against toxic concentrations of hydrogen peroxide using bovine aortic endothelial cells was also investigated.

## Introduction

Over the past decades, nitroxides have been extensively employed as building blocks for the development of molecular magnetic materials<sup>1</sup> and as modulators of polymerization processes.<sup>2</sup> Using electron paramagnetic resonance (EPR) spectroscopy, nitroxides have also been employed as spin probes for the investigation of membrane dynamics,<sup>3</sup> metabolism and oxygenation,<sup>4</sup> pH and redox status in cellular systems.<sup>5</sup> Moreover, nitroxides have been used as contrast agents for magnetic resonance imaging.<sup>6</sup> The therapeutic properties of nitroxides<sup>7</sup> have been gaining attention over recent years since

they exhibit protective properties against toxicity induced by reactive oxygen species in cell cultures<sup>8</sup> and whole animals.<sup>7</sup> However, the mechanism of the antioxidant property of nitroxides is poorly understood, but is believed to be due to their ability to catalytically remove superoxide radical anion ( $O_2^{\bullet-}$ ) *via* an SOD-like dismutation mechanism, and therefore may offer cellular protection from the direct and indirect toxicity of  $O_2^{\bullet-}$ .<sup>9</sup> The SOD-mimetic property of nitroxides could proceed *via* two mechanisms: (1) through reduction of the nitroxide by  $O_2^{\bullet-}$  to its hydroxylamine form and subsequent reoxidation by another molecule of  $O_2^{\bullet-}$  to regenerate the nitroxide; (2) or *via* oxidation of the nitroxide to the oxammonium cation, and subsequent reduction to the nitroxide by another molecule of  $O_2^{\bullet-}$ .<sup>10</sup> Also, worth noting is the ability of nitroxides to react with carbon-, sulfur- and oxygen-centered radicals<sup>10</sup> as well as the ability to oxidize iron(II)<sup>9</sup> or reduce ferryl heme,<sup>11</sup> thereby contributing to their antioxidant efficacy. Moreover, nitroxides have been shown to prevent DNA damage induced by transition metal ions<sup>12</sup> or ionizing radiation,<sup>13</sup> as well as inhibit myeloperoxidase-mediated hypochlorous acid production.<sup>14</sup>

Due to the nitroxide dual property to either act as probe or antioxidant, the selective targeting of nitroxides using specific ligands has been an active field of investigation during the last decade. For example, the triphenylphosphonium group was conjugated to pyrrolidine<sup>15</sup> and piperidine nitroxides<sup>16,17</sup> and has been employed as a mitochondria-target molecule. The accumulation of these targeted nitroxides in the mitochondria was demonstrated using EPR spectroscopy as well as by using a selective triphenylphosphonium electrode. An alternative strategy was employed through the use of gramicidin analogues

<sup>a</sup> Laboratoire de Chimie BioOrganique et des Systèmes Moléculaires Vectoriels, Faculté des Sciences, Université d'Avignon et des Pays de Vaucluse, 33 Rue Louis Pasteur, 84000 Avignon, France.

E-mail: gregory.durand@univ-avignon.fr; Fax: +33 4 9014-4441; Tel: +33 4 9014-4445

<sup>b</sup> Department of Pharmacology, The Davis Heart and Lung Research Institute, College of Medicine, The Ohio State University, Columbus, OH 43210, USA. E-mail: frederick.villamena@osumc.edu; Fax: +1 614-688-0999; Tel: +1 614-292-8215

<sup>c</sup> Chemical Research Center, Institute of Structural Chemistry, H-1025 Budapest, Pusztaszeri 59, Hungary

<sup>d</sup> Center for Biomedical EPR Spectroscopy and Imaging, The Davis Heart and Lung Research Institute, College of Medicine, The Ohio State University, Columbus, OH 43210, USA

† Electronic supplementary information (ESI) available: Materials, general procedures and instrumentation for the synthesis, experimental procedures for **10**, **11**, **13** and **14**; materials and general procedures for cell culturing; <sup>1</sup>H and <sup>13</sup>C spectra of **1**, **2**, **5** and **6**; MS spectra of **2**, **3**, **6**, **7**, **8**, **10** and **13**; HRMS spectra of **4**, **11** and **14**; concentration dependence of nitrogen coupling and linewidth of 3-CP and 4-AT in PBS; X-band EPR spectra of clustered and non-clustered **4** and **11** in PBS; radical distribution as function of the concentration of **4**, **7**, **11** and **14**; nitroxide stability data. See DOI: 10.1039/c0nj00024h

that ensure favorable mitochondrial targeting.<sup>18</sup> On the other hand, membrane-targeted nitroxides in which a lipophilic tail serves as an anchor were synthesized<sup>19,20</sup> and were employed to investigate oxidative stress occurring within the cell.

Several amphiphilic antioxidants have been developed in our group as potential therapeutic agents with the expectation that amphiphilic compounds possessing both hydrophilic and lipophilic groups may exhibit improved cellular permeability.<sup>21–23</sup> Amphiphilic antioxidants are comprised of a hydrophilic polar head which provides water solubility while a hydrophobic tail ensures sufficient lipophilicity to pass through cell membranes. Amphiphilic  $\alpha$ -phenyl-*N*-*tert*-butyl nitron derivatives have shown enhanced protective properties against reactive oxygen species-mediated toxicity in *in vitro*,<sup>22,24</sup> *ex vivo*<sup>25</sup> and *in vivo* models,<sup>26,27</sup> compared to unconjugated nitrones, further validating the effect of amphiphilic group on their protective properties. To extend the concept of amphiphile conjugation to other antioxidants, fluorinated amphiphilic amino acids have been developed.<sup>23,28</sup> Lysine and aspartic acid were used as scaffolds upon which a hydrophilic lactobionamide group and a lipophilic fluorinated chain were grafted to the primary functional groups while the antioxidants were grafted to the side chain. In particular, we have recently reported the synthesis and the cytoprotective properties of the first fluorinated amphiphilic cyclic nitron derivative.<sup>29</sup> Indeed, while amphiphilic compounds endowed with a hydrocarbon chain can destabilize cell membranes when used above their critical micellar concentration (cmc), fluorinated amphiphilic analogues are devoid of such detergent properties.<sup>30</sup> However, our previous findings with amphiphilic nitrones show conflicting results where the LPBNAH which is conjugated to hydrogenated carrier shows greater biological activity compared to its fluorinated analogues,<sup>24,27</sup> suggesting other factors are involved for their bioactivity.

With the goal to prove whether the grafting of a nitroxide with an amphiphilic carrier may affect its bioavailability and bioactivity, we present in this work the synthesis of novel hydrogenated-octyl chain amphiphilic amino acid-based cyclic nitroxides (Fig. 1) designed to provide amphiphilic character to nitroxides without inducing cellular toxicity. Indeed, sugar-based octyl surfactants exhibit relatively high cmc (around 20 mM) so no toxicity should be detected if used below their cmc. Piperidine and pyrrolidine nitroxides using 4-amino-TEMPO (4-AT) and 3-carboxyproxyl (3-CP), respectively, were grafted to the amphiphilic carriers. To investigate the effect of the nature of the chain on the physical-chemical and biological properties of nitroxides, fluorinated amphiphilic amino acid-based nitroxides were also prepared. The self-aggregation properties in aqueous media of these surfactant-like nitroxides were confirmed by dynamic light scattering (DLS) as well as electron paramagnetic resonance (EPR) spectroscopy and were correlated with their respective lipophilicity. The effect of the carrier groups on the electrochemical properties of the nitroxides was also investigated using cyclic voltammetry, and the rates of reduction of the aminoxyl group using ascorbate as reducing agent were measured. Moreover, by comparing the physical-chemical data of TEMPO, 4-AT and its amido derivative 4-Act, (Fig. 1) we pointed out the effect of the substituent. Finally, their cytoprotective property

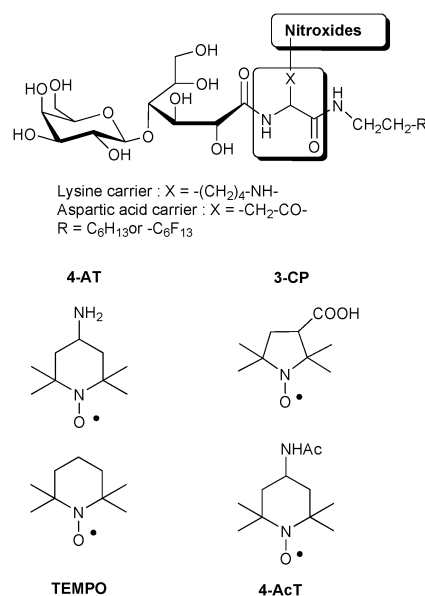


**Fig. 1** Structures of hydrogenated and fluorinated amphiphilic carriers grafted on various types of nitroxides.

against toxic concentrations of hydrogen peroxide using bovine aortic endothelial cells was investigated.

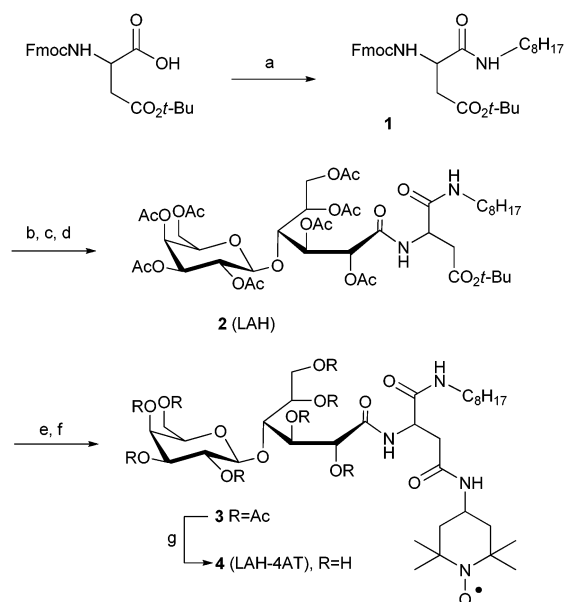
## Results and discussion

### Synthesis

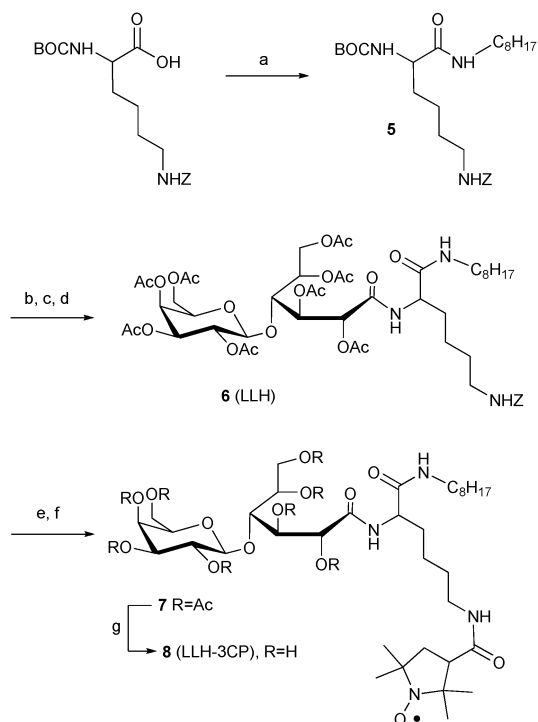
The synthetic strategy for the amphiphilic amino acid nitroxides is based on three key steps: (i) introduction of an alkyl chain on a protected amino acid, (ii) condensation of a lactobionamide polar group on the hydrophobic amino acid derivative, and (iii) conjugation of the nitroxide on the amino acid side chain.

Condensation of octylamine with *N*<sup>α</sup>-(9-fluorenylmethyl-oxy-carbonyl)-L-aspartic acid- $\beta$ -*tert*-butyl ester in the presence of dicyclohexylcarbodiimide (DCC)/hydroxybenzotriazole (HOBt) gave compound **1** with 92% yield (Scheme 1). *N*-Fmoc deprotection was achieved under basic condition in the presence of diethylamine in acetonitrile, and the resulting amino compound was grafted on lactobionolactone, prepared according to our previously described procedure.<sup>23</sup> Acetylation of the crude mixture gave compound **2** with 39% yield in three steps. The *tert*-butoxycarbonyl protective group was removed under acidic conditions in the presence of trifluoroacetic acid in dichloromethane, and condensation of 4-AT on the resulting carboxylic acid derivative was achieved in the presence of 1-ethyl-3-(3-dimethylaminopropyl)carbodiimide (EDC)/HOBt to give, after purification, compound **3** with 46% yield in two steps. Finally, Zemplén de-*O*-acetylation gave the amphiphilic nitroxide **4**.

Condensation of octylamine on *N*<sup>α</sup>-*tert*-butyloxycarbonyl-*N*<sup>ε</sup>-benzyloxycarbonyl-L-lysine in the presence of DCC/HOBt gave **5** with 74% yield (Scheme 2). After *N*-Boc group removal under acidic conditions, the resulting lysine amino intermediate was grafted onto lactobionolactone, followed by acetylation of the hydroxyl groups to give compound **6** in 50% yield in three steps. Benzyloxycarbonyl group removal was achieved by catalytic hydrogenolysis, and the resulting amino compound



**Scheme 1** Synthesis of 4-AT aspartic acid derivative **4**. *Reagents:* (a) octylamine, DCC/HOBt,  $\text{CH}_2\text{Cl}_2$ ; (b) DEA- $\text{CH}_3\text{CN}$  1:9 (v/v); (c) lactobionic acid, TEA, methoxyethanol; (d)  $\text{Ac}_2\text{O}$ -pyridine 1:1 (v/v); (e) TFA- $\text{CH}_2\text{Cl}_2$  4:6 (v/v); (f) **4-AT**, EDC/HOBt,  $\text{CH}_2\text{Cl}_2$ ; (g) MeONa, methanol.



**Scheme 2** Synthesis of 3-CP lysine derivative **8**. *Reagents:* (a) octylamine, DCC/HOBt,  $\text{CH}_2\text{Cl}_2$ ; (b) TFA- $\text{CH}_2\text{Cl}_2$  3:7 (v/v); (c) lactobionic acid, TEA, methoxyethanol; (d)  $\text{Ac}_2\text{O}$ -pyridine 1:1 (v/v); (e)  $\text{H}_2$ , 7 bar, Pd/C, ethanol- $\text{AcOH}$  99:1 (v/v); (f) **3-CP**, EDC/HOBt,  $\text{CH}_2\text{Cl}_2$ ; (g) MeONa, methanol.

was added to 3-CP in the presence of EDC/HOBt to give compound **7** in 32% yield after purification from **6**. Finally, de-*O*-acetylation of **7** led to compound **8**.

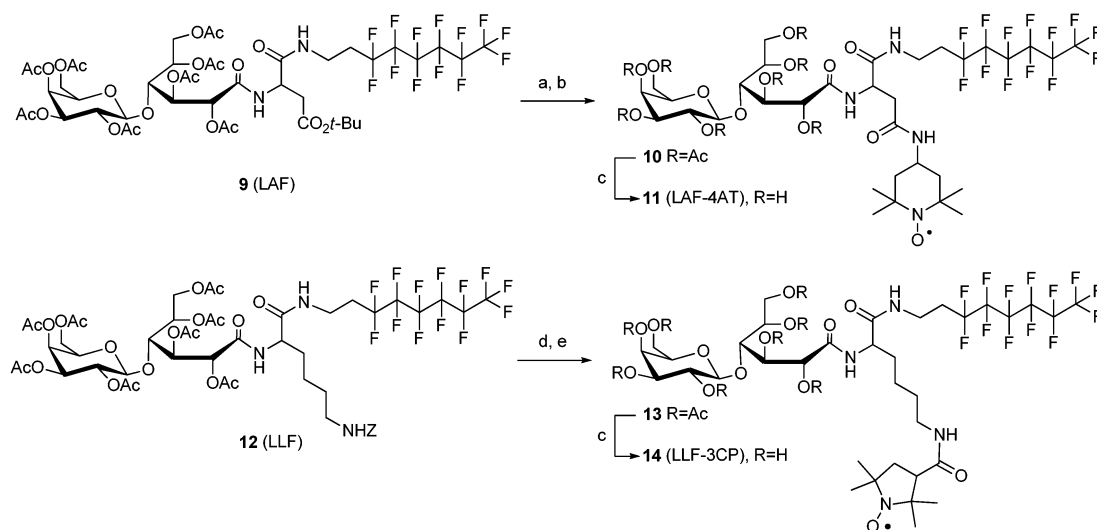
The fluorinated carriers were prepared as previously described by using 1*H*,1*H*,2*H*,2*H*-perfluorooctylamine.<sup>23</sup> Compounds **11** and **14** were prepared following the same procedure employed for **4** and **8**, respectively (Scheme 3). Deprotection of **9** under acidic conditions followed by grafting of the 4-AT in the presence of EDC/HOBt gave compound **10** in two steps in 60% yield. The benzyloxycarbonyl group of **12** was removed by catalytic hydrogenolysis, and the resulting amino compound was added to 3-CP in the presence of EDC/HOBt to give compound **13** in 28% yield. Finally, Zemplén de-*O*-acetylation of **10** and **13** gave the amphiphilic nitroxides **11** and **14**, respectively.

The hydrogenated carriers **2** and **6** were fully characterized by NMR experiments as well as by mass spectrometry, while only the latter characterization was performed on the conjugated compounds **4**, **8**, **11** and **14** (see ESI† for details). As shown in Fig. S3 and S6, the  $^1\text{H}$  NMR spectra of the carriers show the presence of relevant moieties such as the acetyl groups of the polar head at 1.95–2.25 ppm as well as the alkyl chain, with a methyl group at 0.9 ppm and five methylene groups at 1.20–1.40 ppm.  $^{13}\text{C}$  NMR and DEPT experiments allowed us to identify the resonance peaks of the methines and methylenes of the lactobionamide group as well as those of the amino acids. For instance, while the methine group of the acid aspartic carrier is at 49.0 ppm that of the lysine carrier is at 52.7 ppm. The carbonyl carbons of the ester and amide bonds were also observed on the  $^{13}\text{C}$  spectra, confirming the structures of compounds **2** and **6**.

For simplicity in naming, the nitroxides are denoted by abbreviated names indicating their chemical structures. The first letter L stands for lactobionamide group, followed by a second letter indicating the nature of the amino acid, with A for aspartic acid and L for lysine, while the third letter indicates the nature of the alkyl chain, with H for the hydrogenated and F for the fluorinated derivative. For example, LAH-4-AT denotes the hydrogenated aspartic acid derivative bearing the 4-AT nitroxide. A similar nomenclature was used for the carrier devoid of nitroxide moiety.

### Partition coefficients

All the amphiphilic nitroxides obtained are highly soluble in water at 25 mM; however, solutions of fluorinated derivatives **11** and **14** were slightly viscous at this concentration. Their relative lipophilicities ( $\log k'_w$ ) were measured by the HPLC technique as previously used,<sup>22</sup> and the data are shown in Table 1. The values for the parent compounds (*i.e.*, 4-AT and 3-CP) are in good agreement with those obtained by calculation (Table 1). In spite of the high solubility of the conjugates in water, they were found to be more lipophilic than the parent nitroxide compounds. The fluorinated analogues LLF-3-CP and LAF-4-AT exhibited higher lipophilicities than their hydrogenated analogues LLH-3-CP and LAH-4-AT, as demonstrated by their higher  $\log k'_w$  values (Table 1). It appears that the polarity difference between LLH-3-CP and LAH-4-AT is less pronounced than that of the parent compounds. The same observation is true with the fluorinated derivatives. This demonstrates that the lipophilicity of amphiphilic nitroxides is mainly determined by the nature of



**Scheme 3** Synthesis of fluorinated 4-AT and 3-CP derivatives **11** and **14**. *Reagents:* (a) TFA–CH<sub>2</sub>Cl<sub>2</sub> 4 : 6 (v/v); (b) **4-AT**, EDC/HOBt, CH<sub>2</sub>Cl<sub>2</sub>; (c) MeONa, methanol; (d) H<sub>2</sub>, 7 bar, Pd/C, ethanol–AcOH 99 : 1 (v/v); (e) **3-CP**, EDC/HOBt, CH<sub>2</sub>Cl<sub>2</sub>.

**Table 1** Partition coefficients, oxidation potential and relative reduction rate constant of the nitroxides

Nitroxide	log <i>k'</i> <sub>w</sub> <sup>a</sup> (RP-HPLC)	<i>C</i> log <i>P</i>	<i>E</i> <sub>1/2</sub> (ox) <sup>e,f</sup> (mV)	Δ <i>E</i> <sub>p</sub> (ox) <sup>e,g</sup> (mV)	Reduction rate <sup>i</sup>
4-AT	1.1	1.05 <sup>c</sup> , 0.9 <sup>d</sup>	612 ± 7	64 ± 2	—
LAH-4-AT	3.6	— <sup>b</sup>	532 ± 14	58 ± 2	117.0
LAF-4-AT	5.1	— <sup>b</sup>	545 ± 11	60 ± 3	114.1
3-CP	1.4	1.61 <sup>c</sup> , 1.4 <sup>d</sup>	288 <sup>h</sup>	63 <sup>h</sup>	1.0
LLH-3-CP	3.7	— <sup>b</sup>	582 <sup>h</sup>	62 <sup>h</sup>	3.2
LLF-3-CP	5.2	— <sup>b</sup>	664 <sup>h</sup>	60 <sup>h</sup>	3.0
4-AcT	— <sup>b</sup>	0.64 <sup>c</sup> , 1.2 <sup>d</sup>	421 ± 5	65 ± 3	106.7
TEMPO	— <sup>b</sup>	3.04 <sup>c</sup> , 2.6 <sup>d</sup>	402 ± 5	66 ± 4	23.1

<sup>a</sup> This work. <sup>b</sup> Not determined. <sup>c</sup> Data using Chemdraw 8.0 software. <sup>d</sup> Data for the hydroxylamine form of the nitroxides using the online calculator molecular properties on the Molinspiration Web Site ([www.molinspiration.com/cgi-bin/properties](http://www.molinspiration.com/cgi-bin/properties)) as reported by Jiang *et al.*<sup>31</sup> <sup>e</sup> 0.15 M NaCl in water, glassy carbon electrode, sweep rate 0.1 V s<sup>-1</sup>. Average of 4 measurements unless otherwise indicated. <sup>f</sup> *E*<sub>1/2</sub> = (*E*<sub>pc</sub> + *E*<sub>pa</sub>)/2. <sup>g</sup> Δ*E*<sub>p</sub> = *E*<sub>pc</sub> – *E*<sub>pa</sub>. <sup>h</sup> Average of 2 measurements. <sup>i</sup> In the presence of 5 mM ascorbate and determined by EPR. Data are average of two measurements relative to 3-CP.

the carrier, with the lysine derivatives being slightly more lipophilic than the aspartic acid derivatives, which is in perfect agreement with our previous results with PBN derivatives.<sup>23</sup> Therefore, introduction of an amphiphilic character to nitroxides increases their lipophilicity but maintains water solubility.

### Dynamic light scattering

Using dynamic light scattering (DLS) method, the self-aggregation properties of the amphiphilic nitroxides in water was studied. As shown in Fig. 2 and Table 2, all the amphiphilic nitroxides form aggregates with a volume distribution that is strongly dependent on their structure and concentration. At 10 mM, both LAF-4-AT and LLF-3-CP self-organize into well-defined monodisperse particles with ~5.5–6 nm diameter. The amphiphilic PBN derivatives, LLF-PBN and LAF-PBN, were shown to form micelles at concentrations of 0.05 and 0.35 mM.<sup>23</sup> These previous findings, and the similarities in the structures between the fluorinated nitroxides and PBN derivatives, suggest that the aggregates formed by LLF-3-CP and LAF-4-AT at 10 mM are likely spherical micelles, as previously observed for glucose-based fluorinated surfactants.<sup>32</sup>

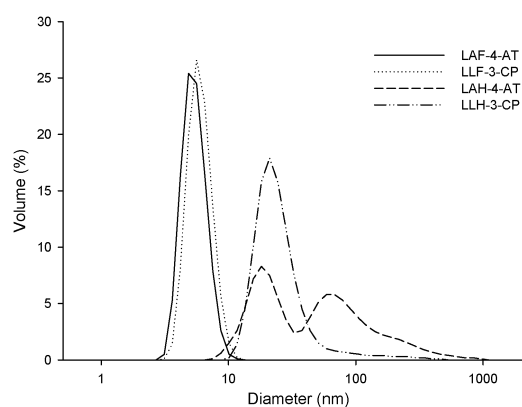


**Fig. 2** Particle size distribution by volume of LAF-4-AT, LLF-3-CP, LAH-4-AT and LLH-3-CP at 10 mM and 25 °C. The graphs report are an average of 8–10 measurements.

Using 20 mM solution of LAH-4-AT, two peaks of ~20 and ~110 nm diameters were observed, indicating the coexistence of two types of particles in almost equal volume distribution, with the latter being very likely polydisperse aggregates. On

**Table 2** Aggregate sizes of amphiphilic nitroxides in aqueous solution

Concentration	LAH-4-AT		LAF-4-AT		LLH-3-CP		LLF-3-CP	
	$D_H^a$	HHW <sup>b</sup>	$D_H^a$	HHW <sup>b</sup>	$D_H^a$	HHW <sup>b</sup>	$D_H^a$	HHW <sup>b</sup>
20 mM	19.0 (59%)	5.1	— <sup>c</sup>	— <sup>c</sup>	29.2	32.5	— <sup>c</sup>	— <sup>c</sup>
	110.9 (41%)	67.8						
10 mM	20.0 (51%)	5.8	5.5	1.2	30.7	35.8	6.0	1.3
	105.1 (49%)	118.7						
5 mM	18.7 (46%)	6.4	5.6	1.2	29.6	37.3	5.9	1.3
	109.0 (53%)	73.7						
1 mM	21.0 (27%)	5.4	21.0 (38%)	6.0	33.6	44.1	5.8	1.2
	108.1 (71%)	71.6	133.6 (57%)	136.2				

<sup>a</sup>  $D_H$ : hydrodynamic diameter of particles of the main peak in nm. The values reported are average of 8–10 measurements. The percentage volume distribution is higher than 98% otherwise mentioned in bracket. <sup>b</sup> HHW, the width of the peak at half-height in nm, which is an indication of the degree of polydispersity of the aggregates. <sup>c</sup> Not determined.

the other hand, LLH-3-CP led to large and polydisperse particles (~30 nm diameter), but with a unimodal distribution. The large and polydisperse particles observed with the hydrogenated derivatives suggest the formation of loose aggregates rather than spherical micelles. Upon dilution, the size and the shape of the particles of the hydrogenated LAH-4-AT and LLH-3-CP do not significantly change, while at 1 mM, phase separation into two particles was observed for LAF-4-AT, similar to that observed for LAH-4-AT. The stronger self-aggregation behaviour of the fluorinated nitroxides is in agreement with their higher lipophilicity as demonstrated by the partition coefficient values (Table 1). It has to be emphasized that below 1 mM, no stable aggregates were observed for any of the compounds.

### Cyclic voltammetry

Cyclic voltammetry (CV) was used to investigate the redox behavior of the amphiphilic nitroxides (200  $\mu$ M) in aqueous solution. As expected, all the nitroxides underwent reversible coupling corresponding to their direct oxidation to the *N*-oxoammonium cation form.

The peak separation ( $\Delta E_p$ ) ranges from 58 to 66 mV, approaching the theoretical Nernstian value (59 mV) and indicating a kinetic reversibility of the oxidation process. The redox potentials ( $E_{1/2}$ ) of the oxidation of the nitroxides were estimated as half of the sum of the anodic ( $E_{pa}$ ) and cathodic peak ( $E_{pc}$ ) potentials, and the data are shown in Table 1. Among the six-membered ring nitroxides, 4-AT gave the highest redox potential ( $E_{1/2} = 612$  mV) while TEMPO gave the lowest ( $E_{1/2} = 402$  mV), indicating facile oxidation for the latter. This is in agreement with previous studies showing substituent effects on the redox potentials.<sup>33,34</sup> Acetylation of the amino group of 4-AT (*e.g.*, 4-AcT) significantly decreased the redox potentials with a value of  $E_{1/2} = 421$  mV, further confirming the effect of the substituent group on the redox potentials, but the presence of amide bond does not significantly alter the redox properties of the nitroxide compared to the non-substituted TEMPO. However, the amphiphilic LAH-4-AT and LAF-4-AT exhibited higher values than the related amido-derivative, 4-AcT. The higher values for the lysinyl 3-CP derivatives LLH-3-CP and LLF-3-CP compared to the 4-AT aspartic acid derivatives are in agreement with the literature, confirming the ease of oxidation of the

six-membered nitroxides.<sup>34</sup> The rationale for the more facile oxidation of six-membered systems was that it was due to a strong pyramidal distortion of the nitroxide moiety leading to a larger spin density on the nitrogen atom.<sup>35</sup> Finally, the redox potentials for all the conjugated nitroxides were found to be higher than the non-conjugated ones. Based on the DLS data presented above, the formation of micellar aggregates at 200  $\mu$ M is not likely to occur for the amphiphilic nitroxides, suggesting that the observed increase in their redox potentials is not due to self-aggregation. However, the steric hindrance provided by the bulky carrier could cause shielding of the nitroxide group, thereby limiting the interaction of the aminoxyl group with the electrode surface and resulting in a more difficult oxidation.

### Relative rates of reduction

The rates of reduction of the amphiphilic nitroxides using ascorbate as reducing agent were measured and were normalized with respect to 3-CP. For comparison, TEMPO, 4-AT and 4-AcT were also included, and the data are shown in Table 1. As described in the literature, the rates of reduction were found to be influenced by the ring size of the nitroxides, with the five-membered ring being less reactive than the six-membered ring nitroxides due to the conformational flexibility of the latter compared to the former.<sup>36,37</sup> Among the pyrrolidine series, the parent compound is three times less reactive than the amphiphilic derivatives, demonstrating that the anionic carboxylate group decreases the reduction rate due to the repulsive interaction between the negatively charged ascorbate and 3-CP. Moreover, no significant difference was observed between the LLF-3-CP and LLH-3-CP, suggesting that the fluorinated chain has no effect on the reduction rate. Among the piperidine series, TEMPO was found to be the less reactive, with a reduction rate constant ~23 times higher than that of 3-CP, while we were unable to determine the reduction rate of 4-AT due to its fast decomposition. The very high reactivity of the amino compound, 4-AT, may be attributed to the electrostatic attraction between the cationic nitroxide and the anionic ascorbate, which supports the previous findings by Morris *et al.*<sup>37</sup> Acetylation of the amino group of 4-AT (*i.e.*, 4-AcT) significantly decreased the reactivity towards ascorbate, with a relative constant of ~107, which is ~5 times higher than the non-substituted TEMPO. This further

confirms that the electron-withdrawing inductive effect of a substituent can increase the reactivity of the nitroxyl group. Moreover, the amphiphilic LAH-4-AT and LAF-4-AT exhibited similar values to their related amido derivative 4-AcT, indicating that the acid aspartic-based carrier, regardless of the nature of the chain, does not affect the reduction rate. However, a slight increase in the reduction rate was observed for the lysinyl derivatives compared to the 3-CP, and this is very likely due to the suppression of repulsive electrostatic interactions. In summary, we found that six-membered nitroxides are more rapidly reduced than the five-membered nitroxides, consistent with the literature,<sup>36,37</sup> and that the nature of the substituent on the nitroxide also affects the reduction rate through the inductive effect and electrostatic interaction with the negatively charged ascorbate. However, the ability of amphiphilic nitroxides to self-aggregate does not seem to alter the reduction rate.

### Electron paramagnetic resonance spectroscopy (EPR) studies

EPR spectroscopy is commonly employed to study the dynamics of complexation or aggregation of paramagnetic species.<sup>38</sup> The nitrogen hyperfine splitting constant ( $a_N$ ) is affected by the polarity around the probe, the pyramidal distortion of the nitroxide moiety as well as the formation of hydrogen bonds with the solvent. An increase in the polarity or hydrogen bonding favours the pseudo-ionic structure B, thus resulting in a higher spin density on the nitrogen and therefore larger  $a_N$  values,<sup>39</sup> while the linewidth broadening results from hindered molecular motion due to microenvironment viscosity, complexation and/or self-aggregation.

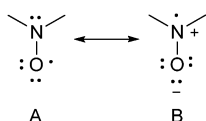


Fig. S21 and S22 show the concentration dependence of the  $a_N$  and linewidths for the unconjugated nitroxides 4-AT and 3-CP. No superimposition of spectral lines was observed and the linewidth varies continuously as a function of concentration. The increase in linewidth and the lowering of  $a_N$  are caused by the encounters between radicals, as evidenced by the quadratic concentration dependence. In both figures, the lines exhibit a perfect parabolic fit. The curvature of the parabolic curve is

larger for 3-CP than for 4-AT, consistent with the faster diffusion of the nitroxide with smaller size.

The effect of concentration on the EPR spectral profiles of the conjugated nitroxides for both hydrogenated and fluorinated carriers grafted to 3-CP and 4-AT were studied, and found to show a different behaviour from that of the unconjugated nitroxides. All spectra can be interpreted as a superimposed signal of a narrow and a broad triplet corresponding to the non-clustered and clustered radicals, respectively. Representative EPR spectra for LLF-3-CP and LLH-3-CP at low and high concentrations are shown in Fig. 3. Similar trends in spectral profile at various concentrations were observed for LAH-4-AT and LAF-4-AT (see Fig. S23 and S24, respectively) but the triplet feature was still evident for LAF-4-AT. For the cluster signal in the hydrogenated carrier,  $a_N$  decreases by *ca.* 0.3 G, while the linewidth increases by 1.3 G (see Table 3). The calculated  $K_1$  from the 2-D simulation of the spectra (see Experimental section for details) gave larger values for the fluorinated compounds compared to the hydrogenated ones, indicating a stronger tendency for aggregation for the former compared to the latter. The larger linewidth and smaller  $a_N$  for the fluorinated nitroxides indicate a stronger magnetic interaction between the nitroxides. This confirms the formation of more compact and smaller aggregates, as already observed by DLS measurements. Moreover, the observed singlet signal for the clustered LLF-3-CP spectrum (Fig. 3) compared to that of LAF-4-AT (Fig. S24) in which the triplet feature is more evident, indicates that stronger magnetic interactions between the nitroxides occurs within the aggregates of LLF-3-CP. This demonstrates that the lysine carrier increases the aggregation compared to the aspartic acid carrier based on the calculated formation constants shown in Table 3. This is consistent with the stronger self-aggregation properties of the lysine derivatives compared to the aspartic acid ones, as demonstrated by size particle measurements and partition coefficients previously obtained in this work. As shown in Fig. 4, the partition of nitroxides between their non-clustered and clustered forms *versus*  $\log[\text{concentration}]$  leads to a sudden change in the slope of the graph for all the nitroxides (see also Fig. S25 for plots as a function of concentration). At this particular concentration, a change in the microenvironment around the nitroxide occurs, which indicates the initial formation of clusters. The change is observed at a concentration lower

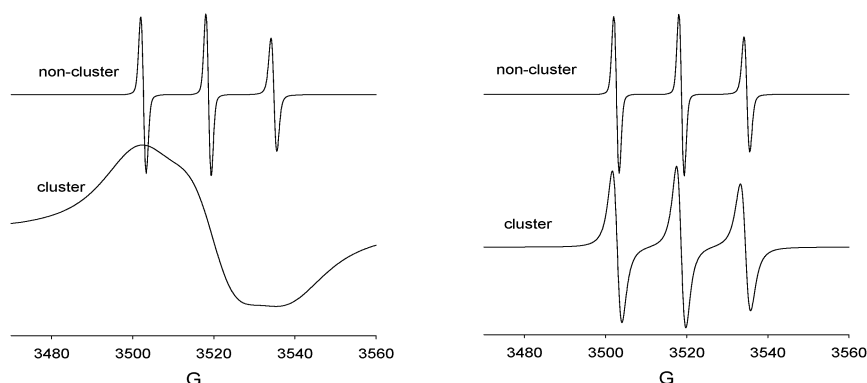
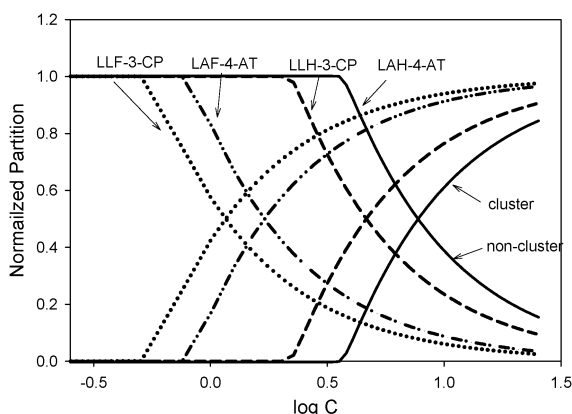


Fig. 3 X-band EPR spectra of the non-clustered and clustered LLF-3-CP (left) and LLH-3-CP (right) in PBS.

**Table 3** EPR parameters and formation constants for LAH-4-AT, LAF-4-AT, LLH-3-CP, and LLF-3-CP in PBS at 298 K

	LAH-4-AT		LAF-4-AT		LLH-3-CP		LLF-3-CP	
	Non-cluster	Cluster	Non-cluster	Cluster	Non-cluster	Cluster	Non-cluster	Cluster
$g$	2.00551	2.00550	2.00549	2.00470	2.00528	2.00533	2.00530	2.00476
$a_N$ (G)	17.06	16.77	17.07	13.59	16.07	15.81	16.08	10.00
$\alpha$ (G)	0.43	1.73	0.44	9.89	0.23	1.50	0.25	7.00
$K_1$ (L mol <sup>-1</sup> )	—	247	—	1109	—	406	—	1642

**Fig. 4** Radical distributions as a function of  $\log C$  showing the varying degrees of aggregation (see also Fig. S25 for plots as a function of concentration).

than 1 mM for LLF-3-CP and LAF-4-AT while those of LAH-4-AT and LLH-3-CP are  $\sim 3.6$  mM and  $\sim 2.1$  mM, respectively, which could be correlated with the critical micellar concentrations.

The micellisation of surfactants has been demonstrated by EPR using nitroxides as probes, and it was shown that in the pre-micellar concentration range, the  $a_N$  values do not change with the surfactant concentration while a decrease of  $a_N$  is observed below the cmc.<sup>39,40</sup> In this case, as the nitroxide moiety is covalently grafted onto the amphiphilic structure, the EPR interpretation could be more complex and further experiments need to be carried out to confirm whether the change observed in the radical distribution actually corresponds to a critical micellar concentration. The nature and the size of the aggregates formed by this novel series of amphiphilic nitroxides will be further investigated in the future by means of neutron and X-ray scattering as well as analytical ultracentrifugation and surface tension measurements.

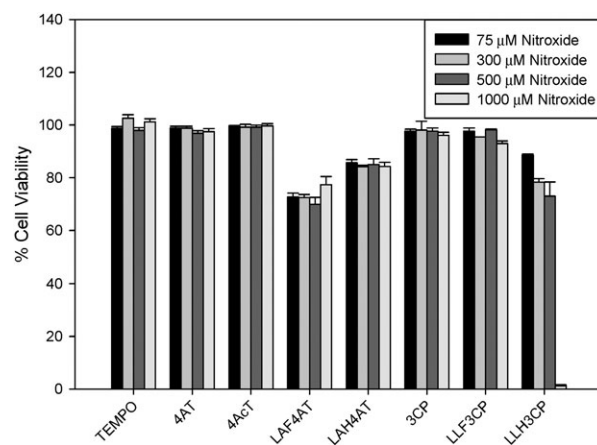
#### Stability of nitroxides with bovine aortic endothelial cells (BAEC)

As shown in Fig. S26, the reduction of 4-AT, TEMPO and LAH-4-AT with ascorbic acid was fully reversed upon treatment with  $K_3[Fe(CN)_6]$  while the very stable 3-CP was not reduced in the presence of ascorbic acid, confirming the reduction rate data presented above. The incubation of these four nitroxides alone (25  $\mu$ M) for 24 h in cell culture media but in the absence of BAEC did not result in any significant decrease in their EPR signal intensity, demonstrating their stability in the cell culture media at 37 °C. However, incubation in the presence of BAEC shows a significant decrease in signal intensity in the extracellular media for 4-AT, LAH-4-AT and TEMPO but

not for 3-CP from 1 h to 24 h. Moreover, addition of 250  $\mu$ M of  $K_3[Fe(CN)_6]$  to convert the possibly formed hydroxylamines back to the nitroxide only gave a small increase in signal intensity for 4-AT and TEMPO but not for LAH-4-AT (Fig. S27). This suggests that 4-AT, LAH-4-AT and TEMPO may have been metabolized intracellularly and/or converted to products other than hydroxylamines, while 3-CP remains likely extracellular due to its anionic nature in solution. In addition, cells lysed after 1 h incubation with 4-AT showed a detectable EPR signal consistent with the permeability of 4-AT compound ( $< 10\%$  relative intensity compared to control, Fig. S27); however, no signal was detected in lysed cells after 24 h, indicating further degradation of the nitroxide.

#### Cytotoxicity of nitroxides

As shown in Fig. 5 using BAEC, the cytotoxicity of the various nitroxides was initially determined in the concentration range of 75–1000  $\mu$ M, and results show that the non-conjugated nitroxides, TEMPO, 4-AT, 4-AcT, 3-CP and LLF-3-CP are non-toxic, in agreement with the literature for the piperidine nitroxides TEMPO, 4-AT and 4-AcT,<sup>41</sup> while LAF-4AT, LAH-4-AT and LLH-3-CP (up to 500  $\mu$ M) were found to induce moderate toxicity (*i.e.*,  $> 70\%$  viability) at the same concentration range. Similar toxicity behavior at high concentrations was observed with an amphiphilic cyclic nitron comprised of the same fluorinated carrier, while the linear nitron derivative was found to be devoid of any toxicity.<sup>29</sup> This confirms that conjugation of certain antioxidants with an amphiphilic carrier may induce a little toxicity at high

**Fig. 5** Cytotoxicity of various nitroxides. Cells were incubated in the presence of nitroxides at concentrations 75, 300, 500 and 1000  $\mu$ M for 24 h. Cell viability was measured using MTT assay (see experimental for details). The  $y$ -axis corresponds to the % viability relative to untreated cells.  $n = 3-5$ .

concentration. In spite of the higher toxicity observed *in vitro* for the pyrrolidine nitroxides compared to the piperidine nitroxides,<sup>12</sup> 3-CP was found to be non-toxic within the concentration range used in this study. The acute toxicity of LLH-3-CP observed at 1000  $\mu\text{M}$  is most likely due to its detergent property, which could result to cell membrane lysis. Indeed, no toxicity was observed with its fluorinated analog at the same concentration.

### Cytoprotective properties

The effect of amphiphilic nitroxides on  $\text{H}_2\text{O}_2$ -treated BAEC was investigated in the concentration range of 75–500  $\mu\text{M}$  and compared to that of the non-conjugated derivatives. We also used the parent compounds 4-AT and 3-CP as controls in order to know whether the amphiphilic-mediated targeting strategy is relevant when used with nitroxides. These parent compounds, however, are expected to be charged in buffer solution that could affect their membrane permeability compared to the neutral conjugated analogues, so we therefore also used the uncharged 4-AcT and TEMPO to discount the charge effects.

In general, the 5-membered ring nitroxides showed no protective effects in the concentration range tested, unlike the 6-membered ring nitroxides (Fig. 6). In addition, varying degrees of protection were observed among the 6-membered ring nitroxides tested, and 4-AT which bears an amino substituent at the C-4 position, was found to be the most protective, followed by the C-4 acetamide substituted compound (4-AcT), and by LAF-4-AT. However, the compounds LAH-4-AT and TEMPO exhibited the lowest protection among the 6-membered ring nitroxides tested. Czepas *et al.*<sup>41</sup> showed that substitution at the C-4 position of piperidine nitroxide is an important parameter affecting its biological property. For example, 4-AcT and 4-AT are more potent than TEMPO and its hydroxylated derivative, TEMPOL, in

preventing hydrogen peroxide-induced cytotoxicity. Moreover, previous studies<sup>41,42</sup> showed that while 4-AT was found to be rapidly reduced to its hydroxylamine form and remains inside the cell in this reduced form, 4-AcT was found to be slowly reduced, and the concentration of its hydroxylamine form in the cell is lower. The absence of antioxidant property of TEMPO was explained by its reduction to its amine form and the weak antioxidant properties of secondary amines.<sup>8</sup> The following trend, in order of decreasing protection of BAEC exposed to lethal concentration of hydrogen peroxide, was observed: 4-AT > 4-AcT > TEMPO, and is similar to those previously observed.

Hydrogen peroxide diffuses through cell membranes, and at unregulated concentrations may induce cellular injury, leading to apoptosis or necrosis.<sup>43,44</sup> The mechanism of antioxidant action of nitroxides (or its reduced hydroxylamine form) against  $\text{H}_2\text{O}_2$ -induced toxicity is not well understood but is believed to be due to its direct reaction with  $\text{HO}^\bullet$  (*via* Fenton reaction). The reported rate constants for these reactions are in the order of  $10^9 \text{ M}^{-1} \text{ s}^{-1}$ ,<sup>45</sup> and the observations by Czepas *et al.*<sup>41</sup> are in agreement with this hypothesis. Moreover, the ability of nitroxides to oxidize low-valent transition metal ions Cu(I) and Fe(II) could also limit the production of  $\text{HO}^\bullet$  *via* a Fenton-type reaction. Also, the fact that cell-permeable nitroxides can prevent DNA damage induced by  $\text{H}_2\text{O}_2$ <sup>13,46</sup> and that nitroxides and hydroxylamines equally prevented DNA damage<sup>45</sup> suggest that the protection offered by nitroxides or its metabolic product (*i.e.*, hydroxylamine) are mostly intracellular in nature.<sup>46</sup> Moreover, nitroxides in fact exhibit anti-apoptotic activity,<sup>31</sup> perhaps through its SOD mimetic activity, oxidation of semiquinone radicals, and modulation of NO levels *via* sequestration of superoxide radical anion. It can therefore be assumed that the antioxidant activity of nitroxides encompasses complex mechanisms that can involve direct or indirect radical reaction with exogenously and endogenously generated radicals during the 24 h of cell treatment with  $\text{H}_2\text{O}_2$ .

As we demonstrated above, the rate of reduction of 4-AT by ascorbate was much faster than those of the other piperidine nitroxides; such an observation could explain the high efficacy of 4-AT against cytotoxicity. In contrast, the pyrrolidine compounds were found to be slowly reduced by ascorbate and exhibited no protective activity. The higher potency of 4-AT compared to its amido derivative 4-AcT indicates that the nature of the substituent plays a major role in cytoprotection. The fact that 4-AcT and LAF-4-AT did not show any significant difference in their protective properties suggests that the amphiphilic group does not play a major role in cytoprotection and that their lipophilicity does not affect their biological activity. This result is quite surprising since we demonstrated that grafting the nitrones PBN and DMPO onto the same fluorinated carrier significantly increases the potency of the parent nitrones in preventing oxidant-induced toxicities.<sup>23,29</sup> Also worth noting is that in our procedure, cells were challenged with  $\text{H}_2\text{O}_2$  24 h after being treated with the nitroxides. This suggests that the protection afforded by the nitroxides could be mostly provided by hydroxylamine<sup>17</sup> (or its metabolic products, where such a scenario is possible during 24 h), and the fact that nitroxides cannot be restored from the cytosolic fractions after 24 h of incubation.

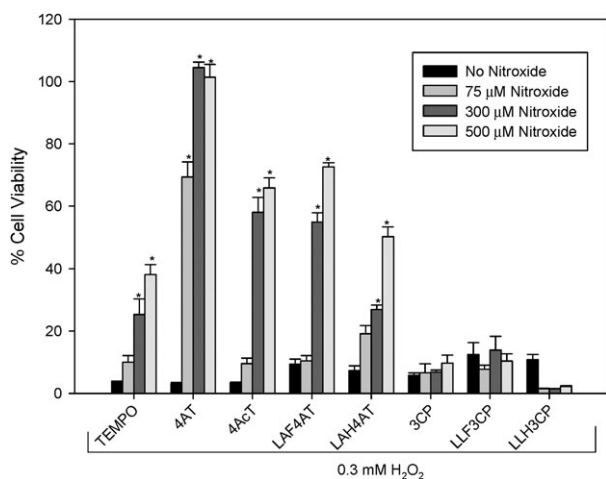


**Fig. 6** Cytoprotective properties of various nitroxides (0, 75, 300 and 500  $\mu\text{M}$ ) against hydrogen peroxide induced cell death. Cells were incubated in the absence or presence of nitroxides for 24 h before being exposed to 300  $\mu\text{M}$  hydrogen peroxide for another 24 h. Cell viability was measured using MTT assay (see Experimental section for details). The y-axis corresponds to the % viability relative to untreated cells. \* Significantly different from 300  $\mu\text{M}$  hydrogen peroxide treatment by t-test,  $p < 0.05$ ,  $n = 2-4$ .

## Conclusions

A novel series of amphiphilic nitroxides possessing a lactobionic polar head, a hydrophobic tail, and an amino acid as scaffold conjugated to 4-amino TEMPO or 3-carboxyproxyl were synthesized. Fluorinated amphiphilic nitroxides LLF-3-CP and LAF-4-AT led to small and monodisperse aggregates of ~5–6 nm diameter while the hydrogenated 3-CP derivative led to larger micellar aggregates of ~30 nm diameter, and its 4-AT derivative led to polydisperse aggregates. The stronger self-aggregation properties of the fluorinated derivatives compared to hydrogenated ones were confirmed by EPR experiments. The large linewidth and small  $a_N$  for the fluorinated nitroxides suggests a more compact cluster where the magnetic interaction between the nitroxides are rather strong. EPR results also show that the lysine carrier increases the clustering compared to the aspartic acid.

Cyclic voltammetry showed that all the nitroxides underwent reversible couple corresponding to their direct oxidation to the *N*-oxoammonium cation form. As previously reported, we observed the ease of oxidation of the six-membered ring nitroxides and that the oxidation potentials being increased upon conjugation to an amphiphilic carrier. The relative rates of reduction of the nitroxides by ascorbate showed that piperidine nitroxides are more rapidly reduced than pyrrolidine, and that the nature of the substituent on the nitroxide also affects the reduction rate through inductive and electrostatic effects. However, no correlation between the amphiphilicity of the nitroxide and the reduction rate was observed. While the six-membered ring nitroxides exhibited cytoprotective activity against H<sub>2</sub>O<sub>2</sub>-induced cell death, the five-membered ring nitroxides showed no protective effect. The order of decreasing cytoprotective ability for the piperidine series is: 4-AT > LAF-4-AT = 4AcT > LAH-4-AT > TEMPO. This suggests that the amphiphilic group does not play a major role in cytoprotection of nitroxide compounds, contrary to what was observed for the nitrones PBN and DMPO, in which grafting onto the fluorinated amphiphilic carrier led to increased cytoprotection by the parent nitron.

## Experimental section

### Syntheses

***N*-(9-Fluorenylmethoxycarbonyl)- $\beta$ -(*tert*-butyloxycarbonyl)-*L*-aspartyl-octylamide (1).** A mixture of octylamine (0.753 g,  $5.83 \times 10^{-3}$  mol), FmocAsp(O*t*Bu)OH (2 g,  $4.86 \times 10^{-3}$  mol), DCC (1.2 g,  $5.83 \times 10^{-3}$  mol), and HOBT in dry CH<sub>2</sub>Cl<sub>2</sub> was stirred for 2 h at room temperature and then concentrated under vacuum. The crude mixture was purified by flash chromatography (EtOAc–cyclohexane 2:8 v/v) to give compound **1** (2.34 g,  $4.47 \times 10^{-3}$  mol, 92%) as a white powder.  $R_f$  0.53 (EtOAc–cyclohexane 4:6 v/v). mp 117 °C.  $[\alpha]_D^{25} + 13.7$  (c 1 in CH<sub>2</sub>Cl<sub>2</sub>).  $\delta_H$ (250 MHz, CDCl<sub>3</sub>) 7.80 (2H, d,  $J = 7.6$  Hz), 7.61 (2H, d,  $J = 7.3$  Hz), 7.47–7.29 (4H, m), 6.48 (1H, m), 5.98 (1H, d,  $J = 7.7$  Hz), 4.47 (3H, m), 4.25 (1H, t,  $J = 6.8$  Hz), 3.26 (2H, m), 2.98–2.53 (2H, m), 1.48 (12H, s), 1.29 (9H, s), 0.9 (3H, t,  $J = 7.1$  Hz).  $\delta_C$ (62.86 MHz, CDCl<sub>3</sub>) 171.3, 170.2, 155.4 (CO), 143.7, 141.3 (C), 127.8, 127.1, 125.0, 120.1, 120.0 (CH), 82.9

(C), 67.1 (CH<sub>2</sub>), 51.1, 47.2 (CH), 39.7, 31.8, 29.5, 29.2 (CH<sub>2</sub>), 28.1 (CH<sub>3</sub>), 26.8, 22.6 (CH<sub>2</sub>), 14.1 (CH<sub>3</sub>).

***N*-(2,3,4,6,2',3',4',6'-*O*-Acetyl-lactobionyl)- $\beta$ -(*tert*-butyloxycarbonyl)-*L*-aspartyl-octylamide (2).** Compound **1** (0.8 g,  $1.53 \times 10^{-3}$  mol) was dissolved in a DEA–CH<sub>3</sub>CN 1:9 (v/v) mixture at room temperature. After 1 h of being stirred, the solvent was evaporated under vacuum to give the corresponding amino derivative as a yellow oil (0.445 g,  $1.49 \times 10^{-3}$  mol, 97%). Lactobionolactone (0.713 g,  $1.99 \times 10^{-3}$  mol), prepared according to a published procedure, and the resulting amino compound were dissolved in 2-methoxyethanol with TEA (pH 8–9). The mixture was stirred at 65 °C under argon for 28 h until complete consumption of the amino derivative. Then, the solvent was evaporated under vacuum and the residue was added to a solution of Ac<sub>2</sub>O–pyridine 1:1 (v/v) at 0 °C. After 12 h of being stirred, the mixture was poured into cold 1 N HCl and extracted with CH<sub>2</sub>Cl<sub>2</sub> (3 $\times$ ). The organic layer was washed with brine, dried over Na<sub>2</sub>SO<sub>4</sub>, and concentrated under vacuum. The crude mixture was purified by flash chromatography (EtOAc–cyclohexane 4:6 v/v) to give compound **2** (0.585 g,  $5.99 \times 10^{-4}$  mol, 40%) as a white foam.  $R_f$  0.40 (EtOAc–cyclohexane 6:4 v/v). mp 48.2–49.3 °C (decomposition).  $[\alpha]_D^{25} + 52.0$  (c 1 in CH<sub>2</sub>Cl<sub>2</sub>).  $\delta_H$ (250 MHz, CDCl<sub>3</sub>) 7.52 (1H, d,  $J = 8.3$  Hz), 6.6 (1H, t,  $J = 5.6$  Hz), 5.49 (1H, m), 5.38 (2H, m), 5.11 (2H, m), 4.99 (1H, m), 4.66–4.52 (3H, m), 4.15–3.98 (5H, m), 3.18 (2H, m), 2.93 (1H, dd,  $J = 3.6, 17.0$  Hz), 2.42 (1H, dd,  $J = 6.4, 17$  Hz), 2.23–1.98 (24H, m), 1.43 (9H, s), 1.25 (12H, s), 0.86 (3H, t,  $J = 6.5$  Hz).  $\delta_C$ (62.86 MHz, CDCl<sub>3</sub>) 172.1, 170.5, 170.2, 170.1, 170.1, 169.7, 169.6, 169.5, 169.2, 168.0 (CO), 101.5 (CH), 81.9 (C), 78.0, 72.3, 71.1, 71.0, 69.8, 69.6, 68.9, 66.9 (CH), 61.4, 61.1 (CH<sub>2</sub>), 49.0 (CH), 39.9, 31.8, 29.3, 29.2 (CH<sub>2</sub>), 28.0 (CH<sub>3</sub>), 26.8, 22.6, (CH<sub>2</sub>) 20.8, 20.7, 20.6, 20.5, 14.1 (CH<sub>3</sub>). MS (ESI+,  $m/z$ ) 977.3 [(M + H)<sup>+</sup>], 994.3 [(M + NH<sub>4</sub>)<sup>+</sup>], 999.3 [(M + Na)<sup>+</sup>], 1015.3 [(M + K)<sup>+</sup>].

***N*-(2,3,4,6,2',3',4',6'-*O*-Acetyl-lactobionyl)- $\beta$ -(4-amido-TEMPO)-*L*-aspartyl-octylamide (3).** At 0 °C, compound **2** (0.500 g,  $5.12 \times 10^{-4}$  mol) was dissolved in a TFA–CH<sub>2</sub>Cl<sub>2</sub> 4:6 (v/v) mixture. After 2 h of being stirred, the solution was concentrated under vacuum to give the corresponding acid derivative as a white powder (0.434 g,  $4.71 \times 10^{-4}$  mol, 92%). The resulting acid derivative (0.3 g,  $3.26 \times 10^{-4}$  mol), EDC (0.075 g,  $3.91 \times 10^{-4}$  mol), 4-AT (0.024 g,  $4.24 \times 10^{-4}$  mol) and a catalytic amount of HOBT were dissolved in dry CH<sub>2</sub>Cl<sub>2</sub> with DIEA (pH = 8–9) under argon. The mixture was stirred for 36 h at room temperature and then the solvent was evaporated under vacuum. The crude mixture was purified by flash chromatography (EtOAc–cyclohexane 7:3 v/v) followed by size-exclusion chromatography (CH<sub>2</sub>Cl<sub>2</sub>–MeOH 1:1 v/v) to give compound **3** (0.174 g,  $1.62 \times 10^{-4}$  mol, 50%) as an orange powder.  $R_f$  0.42 (EtOAc). mp 73.1–74.2 °C (decomposition).  $\lambda_{max}$ (CH<sub>2</sub>Cl<sub>2</sub>)/nm 229. MS (ESI+,  $m/z$ ) 1074.4 [(M + H)<sup>+</sup>], 1096.4 [(M + Na)<sup>+</sup>], 1112.3 [(M + K)<sup>+</sup>].

***N*-Lactobionyl- $\beta$ -(4-amido-TEMPO)-*L*-aspartyl-octylamide (4).** Compound **3** (0.160 g,  $1.49 \times 10^{-4}$  mol) was dissolved under argon in MeOH and a catalytic amount of sodium methoxide was added. The mixture was stirred for 4 h and HCl (1 N) was

added dropwise to neutralize the solution. The solvent was evaporated under vacuum and the crude mixture was purified by size-exclusion chromatography (MeOH) to give compound **4** (0.084 g,  $1.12 \times 10^{-4}$  mol, 90%) as an orange powder.  $R_f$  0.5 (EtOAc–MeOH–H<sub>2</sub>O 7:2:1 v/v/v). mp 88.6–89.4 °C (decomposition).  $[\alpha]_D^{25} + 26.3$  (*c* 1 in MeOH).  $\lambda_{\max}(\text{MeOH})/\text{nm}$  229. HR-MS (ESI+, *m/z*) calcd for C<sub>33</sub>H<sub>62</sub>N<sub>4</sub>O<sub>14</sub> [(M + H)<sup>+</sup>]: 738.4257, found 738.4266.

***N*-(*tert*-Butyloxycarbonyl)-*N*'-(benzyloxycarbonyl)-L-lysinyloctylamide (5).** The synthetic procedure was essentially the same as for compound **1**. A mixture of octylamine (1.22 g,  $9.46 \times 10^{-3}$  mol), BocLys(Z)OH (3 g,  $7.88 \times 10^{-3}$  mol), DCC (1.95 g,  $9.46 \times 10^{-3}$  mol) and a catalytic amount of HOBt in dry CH<sub>2</sub>Cl<sub>2</sub> was stirred for 24 h at room temperature and then concentrated under vacuum. The crude mixture was purified by flash chromatography (EtOAc–cyclohexane 4:6 v/v) to give compound **5** (2.88 g,  $5.86 \times 10^{-3}$  mol, 74%) as a white powder.  $R_f$  0.46 (EtOAc–cyclohexane 5:5 v/v). mp 78 °C.  $[\alpha]_D^{25} - 6.0$  (*c* 1 in CH<sub>2</sub>Cl<sub>2</sub>).  $\delta_{\text{H}}(250 \text{ MHz, CDCl}_3)$  7.34 (5H, s), 6.49 (1H, m), 5.36 (1H, d, *J* = 7.87 Hz), 5.09 (3H, s), 4.05 (1H, d, *J* = 5.91 Hz), 3.19 (4H, m), 1.86–1.11 (6H, m), 1.43 (9H, s), 1.27 (12H, s), 0.88 (3H, t, *J* = 6.52 Hz).  $\delta_{\text{C}}(62.86 \text{ MHz, CDCl}_3)$  172.4, 156.6 (CO), 136.6 (C), 128.5, 128.1 (CH), 80.4 (C), 66.7 (CH<sub>2</sub>), 54.4 (CH), 31.9, 31.8, 29.5, 29.3, 29.2 (CH<sub>2</sub>), 28.2 (CH<sub>3</sub>), 26.9, 25.6, 25.0, 22.7, 22.6 (CH<sub>2</sub>), 14.1 (CH<sub>3</sub>).

***N*-(2,3,4,6,2',3',4',6'-*O*-Acetyl-lactobionyl)-*N*'-(benzyloxycarbonyl)-L-lysinyloctylamide (6).** At 0 °C, compound **5** (2.86 g,  $5.82 \times 10^{-3}$  mol) was dissolved in a TFA–CH<sub>2</sub>Cl<sub>2</sub> 3:7 (v/v) mixture. After 6 h of being stirred, the solvent was evaporated under vacuum to give the corresponding amino derivative (2.13 g,  $5.47 \times 10^{-3}$  mol). The resulting amino derivative (2 g,  $5.13 \times 10^{-3}$  mol) and lactobionolactone (1.90 g,  $5.29 \times 10^{-3}$  mol) were dissolved in 2-methoxyethanol with TEA, and the mixture was stirred at 65 °C under argon for 24 h. Then, the solvent was evaporated under vacuum and the residue was added to a solution of Ac<sub>2</sub>O–pyridine 1:1 (v/v) at 0 °C. After 12 h of being stirred, the mixture was poured into cold 1 N HCl and extracted with CH<sub>2</sub>Cl<sub>2</sub> (3×). The organic layer was washed with brine, dried over Na<sub>2</sub>SO<sub>4</sub>, and concentrated under vacuum. The crude mixture was purified by flash chromatography (EtOAc–cyclohexane 4:6 v/v) to give compound **6** (2.8 g,  $2.62 \times 10^{-3}$  mol, 50%) as a white foam.  $R_f$  0.20 (EtOAc–cyclohexane 6/4: v/v). mp 62 °C (decomposition).  $[\alpha]_D^{25} + 5.4$  (*c* 1 in CH<sub>2</sub>Cl<sub>2</sub>).  $\delta_{\text{H}}(250 \text{ MHz, CDCl}_3)$  7.36 (5H, s), 6.61 (1H, d, *J* = 8.0 Hz), 6.08 (1H, m), 5.54 (1H, m), 5.38 (2H, m), 5.16–5.10 (4H, m), 5.01 (1H, dd, *J* = 3.4, 10.0 Hz), 4.61 (1H, d, *J* = 7.8 Hz), 4.54 (1H, dd, *J* = 2.9 Hz, 12.5 Hz), 4.18 (4H, m), 3.91 (1H, t, *J* = 6.6 Hz), 3.20 (4H, m), 2.24–2.00 (24H, m), 1.90–1.38 (6H, m), 1.28 (12H, s), 0.89 (3H, t, *J* = 6.5 Hz).  $\delta_{\text{C}}(62.86 \text{ MHz, CDCl}_3)$  170.6, 170.5, 170.2, 170.1, 170.0, 169.8, 169.3, 169.2, 167.5, 156.6 (CO), 136.7 (C), 128.5, 128.1, 128.0, 101.7, 77.9, 72.6, 71.1, 70.9, 69.9, 69.3, 68.9, 66.8 (CH), 66.5, 61.2, 61.0 (CH<sub>2</sub>), 52.7 (CH), 39.8, 31.8, 29.4, 29.2, 26.9, 22.6, 22.2 (CH<sub>2</sub>), 20.9, 20.8, 20.7, 20.6, 20.5, 14.1 (CH<sub>3</sub>). MS (ESI+, *m/z*) 1068.4 [(M + H)<sup>+</sup>], 1085.4 [(M + NH<sub>4</sub>)<sup>+</sup>], 1090.4 [(M + Na)<sup>+</sup>], 1106.4 [(M + K)<sup>+</sup>].

***N*-(2,3,4,6,2',3',4',6'-*O*-Acetyl-lactobionyl)-*N*'-(carboxyproxyloctyl)-L-lysinyloctylamide (7).** At 0 °C, compound **6** (0.3 g,  $2.81 \times 10^{-4}$  mol) was dissolved in ethanol–acetic acid 99:1 (v/v) and 0.018 g of 10% Pd/C was added portionwise with stirring. The reaction mixture was exposed to a hydrogen atmosphere for 12 h (8 bars). After filtration of the catalyst through a pad of Celite, the solvent was evaporated under vacuum to give the corresponding amino derivative (0.256 g,  $2.75 \times 10^{-4}$  mol). The resulting amino (0.240 g,  $2.57 \times 10^{-4}$  mol), EDC (0.049 g,  $2.57 \times 10^{-3}$  mol), 3-CP (0.040 g,  $2.15 \times 10^{-3}$  mol) and a catalytic amount of HOBt were dissolved in dry CH<sub>2</sub>Cl<sub>2</sub> with DIEA (pH = 8–9) under argon. The mixture was stirred for 18 h at room temperature and the solvent was evaporated under vacuum. The crude mixture was purified by flash chromatography (EtOAc) and by size-exclusion chromatography (CH<sub>2</sub>Cl<sub>2</sub>–MeOH 1:1 v/v) to give compound **7** (0.076 g,  $0.69 \times 10^{-4}$  mol, 32%) as a yellow foam.  $R_f$  0.33 (EtOAc). mp 98.5–99.4 °C (decomposition).  $[\alpha]_D^{25} + 10.5$  (*c* 1 in CH<sub>2</sub>Cl<sub>2</sub>).  $\lambda_{\max}(\text{CH}_2\text{Cl}_2)/\text{nm}$  231. MS (ESI+, *m/z*) 1102.7 [(M + H)<sup>+</sup>], 1119.7 [(M + NH<sub>4</sub>)<sup>+</sup>], 1124.6 [(M + Na)<sup>+</sup>], 1140.7 [(M + K)<sup>+</sup>].

***N*-Lactobionyl-*N*'-(carboxyproxyloctyl)-L-lysinyloctylamide (8).** Compound **7** (0.060 g,  $5.45 \times 10^{-5}$  mol) was dissolved under argon in MeOH and a catalytic amount of sodium methoxide was added. The mixture was stirred for 4 h and HCl (1 N) was added dropwise to neutralize the solution. The solvent was evaporated under vacuum and the crude mixture was purified by size-exclusion chromatography (MeOH), to give the compound **8** (0.040 g,  $5.23 \times 10^{-5}$  mol, 96%) as a yellow powder.  $R_f$  0.41 (EtOAc–MeOH–H<sub>2</sub>O 7:2:1 v/v/v). mp 118.2–119.4 °C (decomposition).  $[\alpha]_D^{25} + 19.0$  (*c* 0.1 in MeOH).  $\lambda_{\max}(\text{MeOH})/\text{nm}$  231. MS (ESI+, *m/z*) 766 [(M + H)<sup>+</sup>], 783 [(M + NH<sub>4</sub>)<sup>+</sup>], 788 [(M + Na)<sup>+</sup>], 804 [(M + K)<sup>+</sup>].

#### Determination of log*k'*<sub>w</sub> values

Compounds were dissolved in MeOH at 1.0 mg mL<sup>-1</sup> and were injected onto a Microsorb C18 column (250 mm × 4.6 mm, 5 μm). The compounds were eluted at various MeOH and water ratios using a flow rate of 0.8 mL min<sup>-1</sup>. The column temperature was 25 °C, and the UV detector wavelength was  $\lambda = 230 \text{ nm}$ . Linear regression analyses were performed on 3 data points (from 8:2 to 6:4 v/v) for LAH-4-AT, LAF-4-AT, LLH-3-CP and LLF-3-CP ( $r^2 > 0.9992$ ); four points (from 8:2 to 4:6 v/v) for 4-AT and 3-CP ( $r^2 > 0.9979$ ). log*k'* values were calculated by using the equation:  $\log k' = \log((t - t_0)/t_0)$ , where *t* is the retention time of the nitroxide and *t*<sub>0</sub> is the elution time of MeOH, which is not retained on the column.

#### Particle size analyses

The hydrodynamic particle size distributions and polydispersity of amphiphilic nitroxides at different concentrations were determined by using a Zetasizer Nano-S model 1600 (Malvern Instruments Ltd., UK) equipped with a He–Ne laser ( $\lambda = 633 \text{ nm}$ , 4.0 mW). In a typical experiment, stock solutions (10 mM) in milli-Q water (resistivity 18.2 mΩ cm) were prepared and stored at room temperature overnight before the measurements. On the day of the experiment, solutions were passed through a

0.45  $\mu\text{m}$  filter, a low-volume quartz batch volume was filled with 100  $\mu\text{L}$  of the stock solution, and the size of the particles was measured 1 h after filtration, and then solutions were gradually diluted. The time-dependent correlation function of the scattered light intensity was measured at a scattering angle of  $173^\circ$  relative to the laser source. The hydrodynamic radius ( $R$ ) of the particles was estimated from their diffusion coefficient ( $D$ ) using the Stokes–Einstein equation,  $D = k_{\text{B}}T/6\pi\eta R$ , where  $k_{\text{B}}$  is the Boltzmann constant,  $T$  is the absolute temperature, and  $\eta$  is the viscosity of the solvent.

### Cyclic voltammetry

Cyclic voltammetry was performed on a potentiostat and computer-controlled electroanalytical system. Electro-chemical measurements were carried out in a 10 mL cell equipped with a glassy carbon working electrode, a platinum-wire auxiliary electrode, and a Ag/AgCl reference electrode. Solutions were degassed by bubbling with nitrogen gas before recording the voltamograms at a scan rate ( $v$ ) of  $0.1 \text{ V s}^{-1}$ . The nitroxide concentration was 200  $\mu\text{M}$  in double-distilled water and the supporting electrolyte was 0.15 M NaCl.

### EPR spectroscopy

EPR spectra were recorded at room temperature using an X-band spectrometer with high sensitivity resonator. General instrument settings for kinetic experiments were as follows: microwave power, 10 mW; microwave frequency, 9.87 GHz; modulation frequency, 100 kHz; modulation amplitude, 1.0 G; sweep width, 120 G; time constant, 10.240 ms; sweep time, 20.40 s. General instrument settings for concentration dependence experiments were as follows: microwave power, 1 mW; microwave frequency, 9.87 GHz; modulation frequency, 100 kHz; modulation amplitude, 1 G; time constant, 20.5 ms; scan time, 41 s. Measurements were performed using 50  $\mu\text{L}$  capillary tubes.

All kinetic experiments were performed in PBS buffer solution. In a typical experiment, to a solution of nitroxide (0.5 mM), ascorbate (5 mM) was added and kinetic measurement was initiated 40 s after the addition of ascorbate. The decrease in the area of the lowest field peak was monitored by EPR as a function of time over a period of 100–900 s. All the data were the average of two measurements. The rates of reduction were calculated using pseudo-first-order rate law. For the concentration dependence experiments, the nitroxides were dissolved in PBS buffer, sonicated for 5 min, and left to stand for 1 h before measurement.

The concentration effect can be well described by an equilibrium between the non-clustered ( $R$ ) and the clustered radicals ( $R_N$ ).<sup>47</sup> These two species were applied in the 2D- simulation of the spectra according to the following equation:  $N \times R \leftrightarrow R_N$ , with the formation constant expressed as  $K_N = [R_N]/R^N$ , where  $N$  is the number of nitroxides in the cluster. Due to the exponential dependence of  $K_N$  with  $N$ ,  $K_1$  was calculated instead as defined by the relation:  $K_1^{N-1} = K_N$  where  $N - 1$  corresponds to the number of steps to form the cluster from the individual nitroxides. When  $\log K$  is divided by  $N - 1$ , one can obtain the logarithm of the individual step. In this case, one can compare the

stability constants for different species even if the  $N$  values are not the same. The 2-D simulation program decomposes simultaneously a set of superimposed spectra recorded at different concentration of the radicals. In this procedure 10 EPR parameters (*e.g.*,  $g$ -factor,  $a_{\text{N}}$ ,  $\alpha$ ,  $\beta$ ,  $\gamma$  relaxation) of the two species (*i.e.*, non-cluster and cluster) and the  $K_N$  formation constant were adjusted using a simulation program for a set of spectra including 11 spectra with the concentration 0.001, 0.01, 0.05, 0.1, 0.25, 0.5, 1, 2.5, 5, 10 and 25 mM, respectively. The value of  $N$  was varied between 2 and 80 to test which equilibrium gives the best fit. The optimum was found in the range 40–80, but the regression factor showed only a slight variation for large  $N$  values.

### Cell viability and stability studies

**3-[4,5-Dimethylthiazol-2-yl]-2,5-diphenyltetrazolium (MTT) reduction assay.** Cytotoxicity of  $\text{H}_2\text{O}_2$  and cytoprotective properties of the nitroxides was assessed using MTT assay. In a typical experiment, BAEC cells were incubated with nitroxides for 24 h in DMEM supplemented with 0.5% FBS in 24-well culture plates at  $37^\circ\text{C}$ . After incubation, a known concentration of  $\text{H}_2\text{O}_2$  was added to the well plates and incubated for an additional 24 h. A 0.5 mL MTT solution ( $0.45 \text{ mg mL}^{-1}$  MTT in DMEM supplemented with 0.5% FBS) was then added to each well. Cells were incubated for another 2 h at  $37^\circ\text{C}$ . After the 2 h incubation, the media were removed and wells were rinsed once with DPBS. A 0.3 mL mixture of dimethyl sulfoxide, isopropanol and deionized water (1:4:5) was added to each well at room temperature to solubilize the formazan crystals. The dissolved formazan was then transferred into semi-micro cuvettes, and the absorbance was measured at 570 nm using a spectrophotometer.

**Stability studies.** In six-well plates, BAEC cells were incubated with 25  $\mu\text{M}$  of the nitroxide for a period of 1 and 24 h. Cells were collected and lysed by sonication. A portion of the cell culture media and lysates were then transferred to 50  $\mu\text{L}$  capillary tubes and the EPR spectra were recorded at room temperature. A solution of 250  $\mu\text{M}$   $\text{K}_3[\text{Fe}(\text{CN})_6]$  was then added to the remaining media and lysates to restore any reduced compound that was formed, and the EPR spectra was taken again. Signal intensities were obtained for each experiment and were compared to the signal intensity of 25  $\mu\text{M}$  of the respective nitroxides incubated alone for 24 h in the absence of BAEC.

**Statistical analysis.** Statistical analysis was performed using Student's *t*-test. Statistical significance was considered at  $P < 0.05$ .

### Acknowledgements

This work is supported by NIH grant HL081248. The Ohio Supercomputer Center (OSC) is acknowledged for generous computational support of this research. FC is the recipient of a fellowship from the “Région Provence Alpes Côte d’Azur” and Targeting System Pharma.

## References

- G. I. Likhtenshtein, J. Yamauchi, S. Nakatsuji, A. I. Smirnov and R. Tamura, *Nitroxides*, Wiley-VCH, 2008.
- G. Moad, E. Rizzardo and S. H. Thang, *Acc. Chem. Res.*, 2008, **41**, 1133.
- D. Marsh, *Pure Appl. Chem.*, 1990, **62**, 265.
- P. Kuppusamy, M. Chzhan, K. Vij, M. Shteynbuk, D. J. Lefer, E. Giannella and J. L. Zweier, *Proc. Natl. Acad. Sci. U. S. A.*, 1994, **91**, 3388.
- V. V. Khrantsov, I. A. Grigor'ev, D. J. Lurie, M. A. Foster, J. L. Zweier and P. Kuppusamy, *Spectrosc. Int. J.*, 2004, **18**, 213.
- J. F. W. Keana and F. L. Van Nice, *Physiol. Chem. Phys. Med.*, 1984, **16**, 447.
- B. P. Soule, F. Hyodo, K.-I. Matsumoto, N. L. Simone, J. A. Cook, M. C. Krishna and J. B. Mitchell, *Free Radical Biol. Med.*, 2007, **42**, 1632.
- M. C. Krishna, W. DeGraff, O. H. Handovszky, C. P. Sár, T. Kálai, J. Jekó, A. Russo, J. B. Mitchell and K. Hideg, *J. Med. Chem.*, 1998, **41**, 3477.
- J. B. Mitchell, A. Samuni, M. C. Krishna, W. G. DeGraff, M. S. Ahn, U. Samuni and A. Russo, *Biochemistry*, 1990, **29**, 2802.
- M. C. Krishna, D. A. Grahame, A. Samuni, J. B. Mitchell and A. Russo, *Proc. Natl. Acad. Sci. U. S. A.*, 1992, **89**, 5537.
- R. J. Mehlhorn and C. E. Swanson, *Free Radical Res.*, 1992, **17**, 157.
- E. Damiani, L. Greci and P. Hrelia, *Free Radical Biol. Med.*, 2000, **28**, 330.
- J. B. Mitchell, W. DeGraff, D. Kaufman, M. C. Krishna, A. Samuni, E. Finkelstein, M. S. Ahn, S. M. Hahn, J. Gamson and A. Russo, *Arch. Biochem. Biophys.*, 1991, **289**, 62.
- M. D. Rees, S. E. Bottle, K. E. Fairfull-Smith, E. Malle, J. M. Whitelock and M. J. Davies, *Biochem. J.*, 2009, **421**, 79.
- A. Dhanasekaran, S. Kotamraju, C. Karunakaran, S. V. Kalivendi, S. Thomas, J. Joseph and B. Kalyanaraman, *Free Radical Biol. Med.*, 2005, **39**, 567.
- J. Dessolin, M. Schuler, A. Quinart, F. De Giorgi, L. Ghosez and F. Ichas, *Eur. J. Pharmacol.*, 2002, **447**, 155.
- J. Trnka, F. H. Blaikie, R. A. J. Smith and M. P. Murphy, *Free Radical Biol. Med.*, 2008, **44**, 1406.
- P. Wipf, J. Xiao, J. Jiang, N. A. Belikova, V. A. Tyurin, M. P. Fink and V. E. Kagan, *J. Am. Chem. Soc.*, 2005, **127**, 12460.
- S. Ban, H. Nakagawa, T. Suzuki and N. Miyata, *Bioorg. Med. Chem. Lett.*, 2007, **17**, 1451.
- J. Mravljak and S. Pecar, *Tetrahedron Lett.*, 2009, **50**, 567.
- G. Durand, A. Polidori, J.-P. Salles and B. Pucci, *Bioorg. Med. Chem. Lett.*, 2003, **13**, 859.
- G. Durand, A. Polidori, O. Ouari, P. Tordo, V. Geromel, P. Rustin and B. Pucci, *J. Med. Chem.*, 2003, **46**, 5230.
- S. Ortial, G. Durand, B. Poeggeler, A. Polidori, M. A. Pappolla, J. Boeker, R. Hardeland and B. Pucci, *J. Med. Chem.*, 2006, **49**, 2812.
- G. Durand, B. Poeggeler, J. Boeker, S. Raynal, A. Polidori, M. A. Pappolla, R. Hardeland and B. Pucci, *J. Med. Chem.*, 2007, **50**, 3976.
- S. Tanguy, G. Durand, C. Reboul, A. Polidori, B. Pucci, M. Dauzat and P. Obert, *Cardiovasc. Drugs Ther.*, 2006, **20**, 147.
- T. Asanuma, H. Yasui, O. Inanami, K. Waki, M. Takahashi, D. Iizuka, T. Uemura, G. Durand, A. Polidori, Y. Kon, B. Pucci and M. Kuwabara, *Chem. Biodiversity*, 2007, **4**, 2253.
- B. Poeggeler, G. Durand, A. Polidori, M. A. Pappolla, I. Vega-Naredo, A. Coto-Montes, J. Böker, R. Hardeland and B. Pucci, *J. Neurochem.*, 2005, **95**, 962.
- S. Périno, C. Contino-Pépin, S. Jasseron, M. Rapp, J.-C. Maurizis and B. Pucci, *Bioorg. Med. Chem. Lett.*, 2006, **16**, 1111.
- G. Durand, R. A. Prosak, Y. Han, S. Ortial, A. Rockenbauer, B. Pucci and F. A. Villamena, *Chem. Res. Toxicol.*, 2009, **22**, 1570.
- E. Chabaud, P. Barthelemy, N. Mora, J. L. Popot and B. Pucci, *Biochimie*, 1998, **80**, 515.
- J. Jiang, I. Kurnikov, N. A. Belikova, J. Xiao, Q. Zhao, A. A. Amoscato, R. Braslau, A. Studer, M. P. Fink, J. S. Greenberger, P. Wipf and V. E. Kagan, *J. Pharmacol. Exp. Ther.*, 2007, **320**, 1050.
- M. Abła, G. Durand and B. Pucci, *J. Org. Chem.*, 2008, **73**, 8142.
- K. Nakahara, S. Iwasa, J. Iriyama, Y. Morioka, M. Suguro, M. Satoh and E. J. Cairns, *Electrochim. Acta*, 2006, **52**, 921.
- J. P. Blinco, J. L. Hodgson, B. J. Morrow, J. R. Walker, G. D. Will, M. L. Coote and S. E. Bottle, *J. Org. Chem.*, 2008, **73**, 6763.
- J. L. Hodgson, M. Namazian, S. E. Bottle and M. L. Coote, *J. Phys. Chem. A*, 2007, **111**, 13595.
- W. R. Couet, R. C. Brasch, C. Sosnovsky, J. Lukszo, I. Prakash, C. T. Gnewech and T. N. Tozer, *Tetrahedron*, 1985, **41**, 1165.
- S. Morris, G. Sosnovsky, B. Hui, C. O. Huber, N. U. M. Rao and H. M. Swartz, *J. Pharm. Sci.*, 1991, **80**, 149.
- J. H. Freed, in *Theory of Slow Tumbling ESR Spectra for Nitroxides*, ed. L. J. Berliner, Academic, 1976.
- A. M. Tedeschi, G. D'Errico, E. Busi, R. Basosi and V. Barone, *Phys. Chem. Chem. Phys.*, 2002, **4**, 2180.
- E. Szajdzinska-Pietek, K. Sulak, I. Dragutan and S. Schlick, *J. Colloid Interface Sci.*, 2007, **312**, 405.
- J. Czepas, A. Koceva-Chyła, K. Gwoździński and Z. Józwiak, *Cell Biol. Toxicol.*, 2008, **24**, 101.
- C. Kroll, A. Langner and H.-H. Borchert, *Free Radical Biol. Med.*, 1999, **26**, 850.
- S. W. Ryter, H. P. Kim, A. Hoetzel, J. W. Park, K. Nakahira, X. Wang and A. M. K. Choi, *Antioxid. Redox Signaling*, 2007, **9**, 49.
- A. M. Gardner, F.-h. Xu, C. Fady, F. J. Jacoby, D. C. Duffey, Y. Tu and A. Lichtenstein, *Free Radical Biol. Med.*, 1997, **22**, 73.
- S. Xavier, K. Yamada, A. M. Samuni, A. Samuni, W. DeGraff, M. C. Krishna and J. B. Mitchell, *Biochim. Biophys. Acta, Gen. Subj.*, 2002, **1573**, 109.
- A. M. Samuni, W. DeGraff, M. C. Krishna and J. B. Mitchell, *Biochim. Biophys. Acta, Gen. Subj.*, 2001, **1525**, 70.
- A. Rockenbauer, T. Szabó-Plánka, Z. Árkosi and L. Korecz, *J. Am. Chem. Soc.*, 2001, **123**, 7646.